

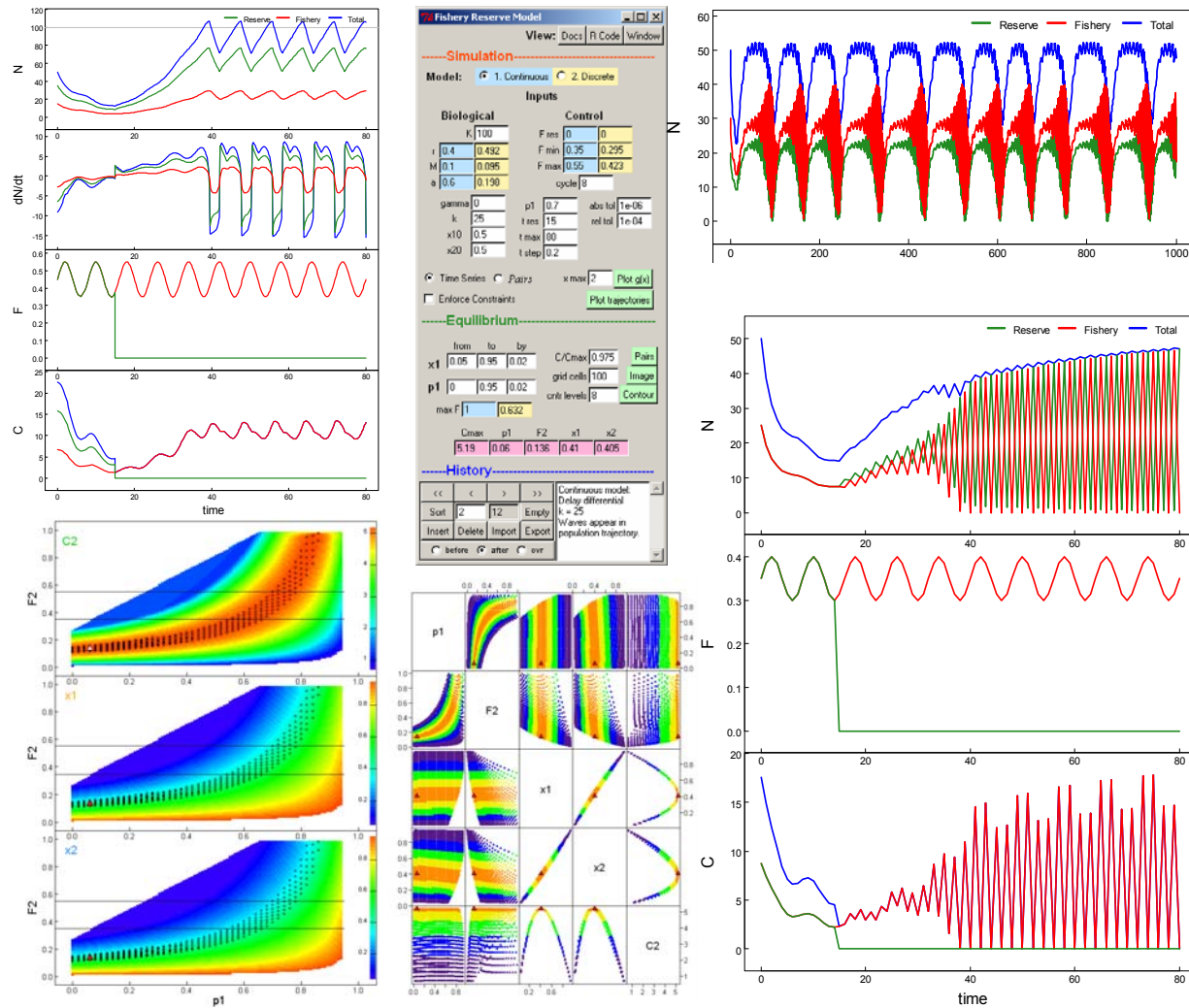
Mathematical Models of Fish Populations in Marine Reserves

Report on a Collaborative Project between Malaspina University-College and the Pacific Biological Station

Jon T. Schnute¹, Rowan Haigh¹, and Alex Couture-Beil²

¹ Fisheries and Oceans Canada, Science Branch, Pacific Biological Station, Nanaimo, B.C.

² B.Sc. 2006. Computing Science Department, Malaspina University-College, Nanaimo, B.C.



Preface

The Pacific Biological Station (PBS) in Nanaimo, BC, conducts research on Canada's Pacific fish stocks and makes scientific recommendations that influence the management of major fisheries in Canada and other nations. Malaspina University-College (MUC), also located in Nanaimo, offers courses in Mathematics and Computing Science that train students for quantitative research. Over the last few years, I've worked collaboratively with Lev Idels (MUC Mathematics) and Jim Uhl (MUC Computing Science) on research projects that facilitate original research and also provide teaching opportunities for MUC students. This report documents work done at PBS on a project to investigate marine reserve models. Lev and I received seed funding from MUC (via a Bamfield Research Grant), along with substantial student support from PBS (via the Groundfish Research Section). We particularly thank David Drakeford (MUC Dean of Science and Technology) and Jeff Fargo (PBS Section Head, Groundfish) for their active interest and support.

We employed the talented MUC student Alex Couture-Beil, who completed the requirements for his B.Sc. degree (Computing Science with a minor in Mathematics) in December, 2006. He worked on this project while he completed his courses, but we were fortunate to retain him through PBS funding for an additional few months. Like other bright MUC students, Alex demonstrated a remarkable ability to learn new ideas quickly, to contribute creatively to project development, and to implement ideas in software. Partly due to his experiences with this research project, he plans to continue with graduate studies in Computing Science.

We designed our research not only to investigate mathematical models of fishery reserves, but also to provide software that allows users to explore the resulting ideas. To make our results widely available, we used the free distribution of the statistical package R (R Development Core Team 2006a). This provides an excellent platform for software development in an environment that supports multiple computers and operating systems. An associated network of contributed libraries on the Comprehensive R Archive Network (CRAN: <http://cran.r-project.org>) gives access to a wealth of algorithms from many users in various fields. The system employs a rigorous testing procedure for all contributed software. Following this disciplined approach, we have now developed the R package *PBS Modelling* that R users anywhere can download from the CRAN web site and use to explore the ideas presented here.

PBS Modelling includes an extensive User's Guide (Schnute et al. 2006) that explains completely how to use the software. It addresses issues that facilitate any modelling process, not just the marine reserves considered here. The user guide, combined with this report, represents more completely the scope of research accomplished at PBS during the course of this project.

Jon Schnute
February 2007

Cover: Graphics from fishery reserve model simulations. See Section 6.

1. Introduction

The recent meeting of the Intergovernmental Panel on Climate Change (IPCC, Paris, January 29 to February 1, 2007; <http://www.ipcc.ch/>) highlights once again the potential effects of human activity on the world's ecosystems. On a smaller scale, fishery managers face more immediate and direct consequences of specific human activities, such as commercial and recreational fishing. Like predictions of global warming due to the release of greenhouse gases, some scientists also predict the collapse of fish populations due to excessive fishing (Pauly et al. 2001; Worm et al. 2006). One proposed solution to this problem involves setting aside marine reserves – regions closed to fishing.

Mathematics offers tools that can help us think systematically about the potential costs and benefits of a plan to implement marine reserves. Unfortunately, systematic thought can be badly flawed if it's based on wrong assumptions. A mathematical model of a biological system represents only a version of reality stemming from the underlying assumptions. At best, it provides a guide to thinking about the consequences of a variety of assumptions, and it can do this only if a spectrum of alternative assumptions are delineated clearly and explored systematically. This report presents such an exploration, based on classical theories of fish population dynamics.

Any model of a marine reserve with an associated fishery must begin with a model of the fishery itself. What was going on before the reserve was established? How might things change afterward? Policy makers must inevitably address such questions. In a marine environment, it is notoriously difficult to figure out what's going on at all. Consequently, anyone making plans for a new management technique has to recognize a high level of uncertainty about the circumstances that preceded the change. It might be difficult to demonstrate that the new technique produced favourable changes or to detect what those changes might be.

An exercise like this one must begin by identifying the key issues. In this report, we focus particularly on the following questions:

1. How do populations change inside and outside a reserve after it is established?
2. How are catches and population levels altered by adjusting the proportion of habitat set aside in the reserve and the level of fishing in the region outside the reserve?
3. What combinations of reserve size and harvest level might be used to achieve social goals, such as a long term stable catch?
4. How are the answers to these questions influenced by the values of key biological parameters, like rates of reproduction, mortality, and migration?

Our mathematical models allow us to explore these questions systematically. We have also designed software tools (discussed in the Preface) that enable stakeholders to conduct their own explorations, and we include examples that illustrate the possibilities.

Although mathematics plays an important role in the material that follows, we're also trying to speak to readers who are not entirely comfortable with mathematical content. We encourage such readers to skim over material that seems troublesome, and move quickly to the graphical illustrations in section 6. We recognize the exercise for what it is – science fiction. The science part comes from mathematics that allows us to explore systematically the consequences of particular assumptions. But the results are fictional, because nature definitely doesn't work

according to such simplistic rules. At best, we can hope to discover patterns that might help us foresee possible outcomes from setting aside marine reserves. Some results can be rather surprising, although perhaps unrealistic. If nothing else, this kind of exploration can be thought provoking and fun. We hope our readers join us in this scientific and playful spirit of inquiry.

2. Fishery Models

We start with two models of fish populations that conform to common ideas from theories of population dynamics. We then apply a simple technique to convert these to reserve models, in which a portion of the environment is set aside as a no-fishing zone. We show that this extension is consistent. Thus, with appropriate starting conditions, the reserve model describes the fishery both before and after the reserve is established.

Classical fish population models often contain three key parameters, a reproductive growth rate r , a mortality rate M , and a carrying capacity K . The parameters r and M signify the potential to reproduce enough to compensate for mortality, with a natural constraint that $r > M$. The parameter K represents environmental limits that constrain growth. The fishery models F1 and F2 in Table 1 encapsulate these ideas, where the associated function $g(x)$ represents density dependence. The argument

$$x_t = N_t / K \quad (2.1)$$

of the function $g(x)$ represents a scaled version of the population N_t of fish at time t , essentially a density relative to the carrying capacity K . Technically, $g(x)$ can also include a vector θ of parameters other than K , so we sometimes write the function in a conditional form: $g(x|\theta)$. We assume that $g(x|\theta)$ is a strictly decreasing function of x for any fixed choice of θ . Biologically, this corresponds to a reduced rate of reproduction per animal as the population N increases.

Model F1 uses a delay differential equation (F1.1) to represent the adult population N_t as a function of continuous time t , influenced by the *instantaneous* natural mortality M and fishing mortality F_t . We assume that M is a fixed parameter associated with fish biology, but that the fishing mortality F_t imposed by the fishery can vary with time. These two sources of mortality occur simultaneously and have an immediate influence on the rate of change of abundance dN/dt . A nonlinear recruitment process involves the function $g(x)$, where a time lag k occurs between larval production and adulthood at age k . The delay differential equation (F1.1) expresses the combined results of adult mortality, recruitment, and fishing. When $k = 0$, it becomes an ordinary differential equation, in which recruitment occurs simultaneously with mortality and fishing.

The function $g(x)$ in (F1.1) decreases from 1 to zero as x increases upward from 0. The specific value $g(1) = M/r$ in (F1.4) guarantees that $N_t = K$ is a constant solution when no fishing mortality occurs ($F_t = 0$). This establishes the intended biological meaning for K , a natural constant level for a pristine population. The constraint (F1.3) deals with a biological limitation mentioned above. To survive at low levels of abundance ($N_t \approx 0$), a population must produce enough recruitment to compensate for natural mortality ($r > M$).

Table 1. Fishery models based on continuous (F1) or discrete (F2) time t . Parameters include a reproductive growth rate r , carrying capacity K , and natural mortality M . Larvae born at time $t - k$ become recruited as adults at the later time t , where recruitment is instantaneous if $k = 0$. Population trajectories are influenced by a time-varying fishing mortality F_t . The state variable $x_t = N_t / K$ defined in (2.1) represents population density per unit of carrying capacity.

Model F1

$$\frac{dN_t}{dt} = -MN_t + rN_{t-k}g\left(\frac{N_{t-k}}{K}\right) - F_t N_t \quad (\text{F1.1})$$

$$\frac{dx_t}{dt} = -Mx_t + rx_{t-k}g(x_{t-k}) - F_t x_t \quad (\text{F1.2})$$

$$0 < M < r \quad (\text{F1.3})$$

$$g(0) = 1, \quad g(1) = \frac{M}{r}, \quad \lim_{x \rightarrow \infty} g(x) = 0 \quad (\text{F1.4})$$

Model F2

$$N_{t+1} = N_t - MN_t + rN_{t-k}g\left(\frac{N_{t-k}}{K}\right) - F_t N_t \quad (\text{F2.1})$$

$$x_{t+1} = x_t - Mx_t + rx_{t-k}g(x_{t-k}) - F_t x_t \quad (\text{F2.2})$$

$$0 < r, \quad 0 < M < \min(1, r) \quad (\text{F2.3})$$

Model F2 expresses a dynamic system similar to F1, but with discrete time steps $t = 0, 1, 2, \dots$. Formally, the difference equation (F2.1) comes from (F1.1) and the derivative approximation

$$\frac{dN_t}{dt} \approx \frac{N_{t+\Delta t} - N_t}{\Delta t} \Big|_{\Delta t=1} = N_{t+1} - N_t, \quad (2.2)$$

where the final term “ $-N_t$ ” has been moved to the right side of (F2.1). Although models F1 and F2 look very similar to each other, the quantities in them have somewhat different interpretations. Technically, r , M , and F_t in (F1.1) are rates per unit time that can take arbitrary positive values. By contrast, M and F_t in (F2.1) represent dimensionless *fractions* of the population removed by natural and fishing mortality during the unit time step from t to $t+1$. Quantities from the two models have the natural relationships

$$r'' = e^{r'} - 1, \quad M'' = 1 - e^{-M'}, \quad F_t'' = 1 - e^{-F_t'}, \quad (2.3a)$$

$$r' = \log(1 + r''), \quad M' = -\log(1 - M''), \quad F_t' = -\log(1 - F_t''), \quad (2.3b)$$

where prime and double prime symbols indicate models F1 and F2, respectively. The constraint (F2.3) reflects the fact that M is a fraction in model F2 ($0 < M < 1$).

Table 2. Example of a function $g(x)$ used to model density dependence in the fishery models F1 and F2 (Table 1). The parameter γ (which can be positive, negative, or zero) influences the shape of this strictly decreasing function, which satisfies the constraints (F1.4). The function $g(x)$ decreases from 1 to 0 as x increase from 0 to ∞ if $\gamma \geq 0$, or as x increases through the finite interval $[0, x_c]$ if $\gamma < 0$, where x_c is defined in (G.2). Formula (G.3) shows an explicit inverse for the function $y = g(x)$.

$$g(x | r, M, \gamma) = \left\{ 1 + \left[\left(\frac{r}{M} \right)^\gamma - 1 \right] x \right\}^{-1/\gamma} \xrightarrow{\gamma \rightarrow 0} \left(\frac{M}{r} \right)^x \quad (\text{G.1})$$

$$g(x | r, M, \gamma) = 0 \text{ if } \gamma < 0 \text{ and } x \geq x_c = \left[1 - \left(\frac{r}{M} \right)^\gamma \right]^{-1} \quad (\text{G.2})$$

$$g^{-1}(y | r, M, \gamma) = \frac{y^{-\gamma} - 1}{\left(\frac{r}{M} \right)^\gamma - 1} \xrightarrow{\gamma \rightarrow 0} \frac{\log y}{\log \left(\frac{M}{r} \right)} \quad (\text{G.3})$$

In the discussion that follows, we use the notation F^* to refer to a model in Table 1, so that the asterisk denotes either number 1 or 2. As mentioned earlier, each dynamic equation ($F^*.1$) represents a density dependent recruitment response with a strictly decreasing function $g(x)$ scaled so that $g(0) = 1$. Divide ($F^*.1$) by K to obtain ($F^*.2$), an equation in the density variable x_t defined in (2.1). This no longer involves K , and the equivalent trajectories

$$x_t = 1 \Leftrightarrow N_t = K \quad (2.4)$$

solve ($F^*.1$) and ($F^*.2$) when there is no fishing ($F_t = 0$). We extend this result in

Theorem 1. In the absence of fishing mortality ($F_t = 0$), both models in Table 1 have the constant solution (2.4). Furthermore, even in the presence of fishing, a trajectory N_t scales to the carrying capacity K . More precisely, given a particular model and a harvest function F_t , suppose that N_{it} is a trajectory with carrying capacity K_i ($i = 1, 2$), where all other parameters are the same. Then if the relationship

$$\frac{N_{1t}}{N_{2t}} = \frac{K_1}{K_2} \quad (2.5)$$

holds during the initial time period ($0 \leq t \leq k$), it persists for all future time $t > k$.

Proof. The proof isn't difficult. The densities $x_{it} = N_{it} / K_i$ ($i = 1$ or 2) both follow exactly the same dynamic equation ($F^*.2$). Furthermore, by assumption (2.5), the densities x_{it} are equal during the initial time period. Consequently, based on the existence and uniqueness of solutions for ($F^*.2$), $x_{1t} = x_{2t}$ for all time t . If x_t denotes this common solution, then $N_{it} = K_i x_t$, a result that proves (2.5) for $t > k$. Existence and uniqueness follow by mathematical induction for

model F2, but are beyond the scope of this paper for model F1. We confine ourselves to the biologically meaningful circumstances in which (F*.1) and (F*.2) have solutions that exist and are unique for specified initial conditions, as illustrated in Section 6. ▀

Table 2 gives explicit formulas for a function $g(x)$ that meet requirements specified in (F1.4). It depends on the model parameters r and M , as well as an extra parameter γ that influences the curve shape. The function (G.1) is designed so that γ can be positive or negative, with definite limiting value as $x \rightarrow 0$. If $\gamma \geq 0$, $g(x)$ is strictly decreasing with an asymptotic limit 0 as $x \rightarrow \infty$. If $\gamma < 0$, $g(x)$ decreases from 1 to 0 as x increases through the finite interval $[0, x_c]$, where x_c is the critical value defined in (G.2) with $g(x_c) = 0$. For larger values of x we define $g(x) = 0$, as in (G.2). The function $y = g(x)$ has an inverse $x = g^{-1}(y)$ given by (G.3), where $g^{-1}(0) = x_c$ if $\gamma < 0$.

We have designed our fishery models explicitly to consider recruitment lags because reserves might sometimes be chosen to ensure larval production. For example, Hastings and Botsford (1999) examined the possibility that a reserve might provide a steady source of larval recruitment into the fishery. Our example in Table 2 follows models proposed by Schnute and Richards (2002), with suitable changes here for lagged models. Some special cases of (G.1) correspond to classical examples that have played significant roles in the historical development of population dynamics. For example, model F1 with no time lag ($k = 0$) and the choice $\gamma = -1$ in (G.1) corresponds roughly to a production model applied to tuna populations by Schaeffer (1954, 1957). Later, Pella and Tomlinson (1969) adopted a similar model with a shape parameter γ . Similarly, Ricker (1954, 1975) and Beverton and Holt (1957) proposed models similar to F2 with $\gamma = 0$ and $\gamma = -1$, respectively.

Our delay differential equation (F1.1) differs in two notable respects from the ordinary differential equations in classical fishery literature. First, it distinguishes recruitment from natural mortality, processes that were often combined historically. This feature requires us to introduce a time delay k that mimics the period of larval development. Second, our version requires the constraint that $g(x) \geq 0$, because recruitment cannot produce negative fish. This means that we have to alter classical models in one other respect to account for both mortality and recruitment.

We illustrate this modification with a simple example. Schaeffer's (1954, 1957) model

$$\frac{dN_t}{dt} = rN_t \left(1 - \frac{N_t}{K} \right) - F_t N_t \quad (2.6)$$

utilized the differential equation for logistic growth. By contrast, our model (F.1a) with $\gamma = -1$ becomes

$$\frac{dN_t}{dt} = -MN_t + rN_{t-k} \max \left[1 + \left(\frac{M}{r} - 1 \right) \frac{N_{t-k}}{K}, 0 \right] - F_t N_t, \quad (2.7)$$

where the function “max” assures positive recruitment. When $k = 0$ and $M = 0$, the differential equation (2.7) reduces to

$$\frac{dN_t}{dt} = rN_t \max \left[1 - \frac{N_t}{K}, 0 \right] - F_t N_t, \quad (2.8)$$

a model identical to (2.6) when $N_t \leq K$. Strictly speaking, (2.8) is not a special case of our model F1 because it violates the constraint $M > 0$, but the distinction between (2.6) and (2.8) highlights a key point. The classical model (2.6) causes the population to decline ($dN_t / dt < 0$) whenever abundance exceeds carrying capacity ($N_t > K$). In our model (2.7), the population constantly experiences natural mortality at the rate M , and a positive recruitment rate must compensate for this loss. In the absence of fishing, both models (2.6) and (2.7) predict that abundance will move toward carrying capacity, but the dynamical reasons for this prediction are different.

3. Reserve Models

Imagine a scenario in which a fishery operates throughout a region with carrying capacity K , where one of the fishery models in Table 1 applies. Suppose that the region is split into two parts with carrying capacities $K_i = p_i K$ ($i = 1, 2$), where $p_1 + p_2 = 1$. We want to use region 1 as a reserve without fishing and allow a fishery only in region 2. At the planning stage, we've only drawn an imaginary boundary in the sea, so our model from Table 1 should remain the same. However, when fishing actually stops in the reserve ($F_{1t} = 0$), our management policy splits the population into two groups. Table 3 presents reserve models (R1, R2) that extend the fishery models (F1, F2) in Table 1 by describing the population dynamics of linked populations N_{1t} and N_{2t} in the reserve and the fishery, respectively.

The mathematical formalism in Table 3 includes two state variables

$$x_{it} = \frac{N_{it}}{K_i} = \frac{N_{it}}{p_i K} \quad (i = 1, 2) \quad (3.1)$$

that represent the abundance density in region i relative to the available carrying capacity. These define two additional state variables:

$$x_t = p_1 x_{1t} + p_2 x_{2t}, \quad y_t = x_{1t} - x_{2t}, \quad (3.2)$$

where x_t and y_t represent an average density and a difference of densities inside and outside the reserve. From (3.1), $p_i x_{it} = N_{it} / K$; consequently the definition (3.2) implies that

$$x_t = \frac{N_{1t} + N_{2t}}{K},$$

so that x_t also represents the density of the total population relative to the total carrying capacity K . The transformation (3.2) between (x_{1t}, x_{2t}) and (x_t, y_t) has an inverse:

$$x_{1t} = x_t + p_2 y_t, \quad x_{2t} = x_t - p_1 y_t. \quad (3.3)$$

Each reserve model (R*.1) in Table 3 looks identical to the corresponding fishery model (F*.1), except for a new term

Table 3. Reserve models for continuous (R1) or discrete (R2) time t , based on the fishery models in Table 1. These models split the original fishery into two parts, where indices $i = 1$ and $i = 2$ correspond to the reserve and fishing zones, respectively. After the reserve is established, $F_{1t} = 0$. Each model represents two equations (with $i = 1, 2$), where j denotes the index opposite to i ($j \neq i$). The proportion p_i represents the fraction of carrying capacity K in zone i , where $K_i = p_i K$ and $p_1 + p_2 = 1$. The parameter a sets a scale for the migration rate, as discussed in the context of (3.4). Biological realism requires the constraints (R1.3) and (R2.3). State variables $x_{it} = N_{it} / K_i$ represent the population density relative to available carrying capacity in zone i .

Model R1

$$\frac{dN_{it}}{dt} = -MN_{it} + rN_{i,t-k} g\left(\frac{N_{i,t-k}}{p_i K}\right) + a\left(\frac{N_{jt}}{p_j} - \frac{N_{it}}{p_i}\right) - F_{it}N_{it} \quad (\text{R1.1})$$

$$\frac{dx_{it}}{dt} = -Mx_{it} + rx_{i,t-k} g(x_{i,t-k}) + \frac{a}{p_i} (x_{jt} - x_{it}) - F_{it}x_{it} \quad (\text{R1.2})$$

$$a > 0 \quad (\text{R1.3})$$

Model R2

$$N_{i,t+1} = N_{it} - MN_{it} + rN_{i,t-k} g\left(\frac{N_{i,t-k}}{p_i K}\right) + a\left(\frac{N_{jt}}{p_j} - \frac{N_{it}}{p_i}\right) - F_{it}N_{it} \quad (\text{R2.1})$$

$$x_{i,t+1} = x_t - Mx_{it} + rx_{i,t-k} g(x_{i,t-k}) + \frac{a}{p_i} (x_{jt} - x_{it}) - F_{it}x_{it} \quad (\text{R2.2})$$

$$0 < a < p_1 p_2 \quad (\text{R2.3})$$

$$m_{ji} = a\left(\frac{N_{jt}}{p_j} - \frac{N_{it}}{p_i}\right) = aK(x_{jt} - x_{it}) \quad (3.4)$$

that represents migration from region j to region i , where $j \neq i$. The migration term (3.4) gives a positive movement from region j to region i when the density in region j is higher than in region i . The additional parameter $a > 0$ sets a scale for the migration rate.

As discussed earlier for parameters r and M , the migration parameter a is a rate for model R1 but a dimensionless fraction for model R2. In this case, the relationship comparable to (2.3) is

$$a'' = p_1 p_2 \left[1 - \exp\left(-\frac{a'}{p_1 p_2}\right) \right], \quad a' = -p_1 p_2 \log\left[1 - \frac{a''}{p_1 p_2}\right], \quad (3.5)$$

where prime and double prime symbols indicate models R1 and R2, respectively. The biological constraints (R1.3) and (R2.3) make these associations consistent with each other.

Table 4. Models with only the movement component for continuous (M1) or discrete (M2) time t , based on the fishery reserve models in Table 3 with $M = r = F_{1t} = F_{2t} = 0$. Model (M*.1) comes from model (R*.2) for the state variables (x_{1t}, x_{2t}) . The transformations (3.2)–(3.3) imply that model (M*.1) is equivalent to (M*.2) for the state variables (x_t, y_t) . The solutions (M*.3) follow easily from model (M*.2). Finally, (M*.3) yields the solution (M*.4) for (x_{1t}, x_{2t}) in model (M*.1). Solutions depend on the initial states $x_0 = p_1 x_{10} + p_2 x_{20}$ and $y_0 = x_{10} - x_{20}$.

Model M1

$$\frac{dx_{1t}}{dt} = \frac{a}{p_1} (x_{2t} - x_{1t}), \quad \frac{dx_{2t}}{dt} = \frac{a}{p_2} (x_{1t} - x_{2t}) \quad (\text{M1.1})$$

$$\frac{dy_t}{dt} = -\frac{a}{p_1 p_2} y_t \quad (\text{M1.2})$$

$$y_t = \exp\left[-\frac{at}{p_1 p_2}\right] y_0 \quad (\text{M1.3})$$

$$x_{1t} = x_0 + p_2 \exp\left[-\frac{at}{p_1 p_2}\right] y_0, \quad x_{2t} = x_0 - p_1 \exp\left[-\frac{at}{p_1 p_2}\right] y_0 \quad (\text{M1.4})$$

Model M2

$$x_{1,t+1} = x_{1t} + \frac{a}{p_1} (x_{2t} - x_{1t}), \quad x_{2,t+1} = x_{2t} + \frac{a}{p_2} (x_{1t} - x_{2t}) \quad (\text{M2.1})$$

$$y_{t+1} = \left(1 - \frac{a}{p_1 p_2}\right) y_t \quad (\text{M2.2})$$

$$y_t = \left(1 - \frac{a}{p_1 p_2}\right)^t y_0 \quad (\text{M2.3})$$

$$x_{1t} = x_0 + p_2 \left(1 - \frac{a}{p_1 p_2}\right)^t y_0, \quad x_{2t} = x_0 - p_1 \left(1 - \frac{a}{p_1 p_2}\right)^t y_0 \quad (\text{M2.4})$$

Table 4 gives a rationale for the associations (3.5). The reserve models R* in Table 3 with $M = r = F_{1t} = F_{2t} = 0$ imply the linear movement models M*, where as usual the asterisk can denote either 1 or 2. When expressed in terms of the state variables (x_t, y_t) in (3.2), these models take the simple form (M*.2) with explicit solutions (M*.3). The transition (3.3) back to density state variables (x_{1t}, x_{2t}) then gives the solutions (M*.4). In particular, the expression

$\exp\left[-\frac{a'}{p_1 p_2}\right]$ in (M1.4) corresponds to $\left(1 - \frac{a''}{p_1 p_2}\right)$ in (M2.4). This correspondence implies (3.5).

Calculations in Table 4 exploit the identity $\frac{1}{p_1} + \frac{1}{p_2} = \frac{p_1 + p_2}{p_1 p_2} = \frac{1}{p_1 p_2}$.

The movement models in Table 4 have a straightforward biological interpretation. The first formulation (M*.1) pertains to the population densities (x_{1t}, x_{2t}) inside and outside the reserve. The second formulation (M*.2) shows that the mean density x_t in (3.2) remains constant and the density difference y_t declines exponentially, given the constraints (R*.3) on a . Mathematically, the transformations (3.2) uncouple the linked system (M*.1) for (x_{1t}, x_{2t}) to produce independent equations (M*.2) for (x_t, y_t) . The final solution (M*.4) says that both x_{1t} and x_{2t} converge to the initial mean density x_0 , where a correction proportional to the initial density difference y_0 declines exponentially toward 0 as $t \rightarrow \infty$.

The solutions (M*.4) to models (M*.1) exist even if the constraints (R*.3) are violated. For example, (M1.4) grows exponentially if $a < 0$. Furthermore, (M2.4) remains bounded if $a < 2p_1p_2$, but oscillates for values a in the range $p_1p_2 < a < 2p_1p_2$. Examples in section 6 illustrate some of the possibilities for these seemingly anomalous cases.

As mentioned in the first paragraph of Section 2, we need to show that the models in Table 3 are consistent with their counterparts in Table 1 during the time period prior to the reserve. Theorem 1 points to the extra assumption required. If we assume a constant fish density relative to local carrying capacity throughout the entire region prior to establishing the reserve, then the condition (2.5) applies to *any* decomposition of the original area. This idea leads to

Theorem 2. The reserve models R* in Table 3 agree with their counterparts F* in Table 1 if the initial populations N_{it} ($i=1, 2$) have a uniform density distribution (2.5) during the initial time period ($0 \leq t \leq k$) and the same harvest function F_t applies in both regions. In particular, the total population $N_t = N_{1t} + N_{2t}$ follows the relevant model F* in Table 1 and the trajectories maintain the constant ratio

$$N_{1t} : N_{2t} : N_t = K_1 : K_2 : K = p_1 : p_2 : 1. \quad (3.6)$$

Proof: We focus on the equations (F*.2) and (R*.2) for the densities x_{it} , which are equivalent to the models (F*.1) and (R*.1) for the populations N_{it} , given the definitions (3.1). First, consider two independent solutions x'_{it} ($i=1, 2$) to the independent models (F*.2). By assumption, these are equal for the initial period and consequently (by Theorem 1) for all time t during which $F_{1t} = F_{2t}$, that is,

$$x'_{1t} = x'_{2t} \equiv x'_t, \quad (3.7)$$

where x'_t is defined by the common value of solutions x_{1t} and x_{2t} . Furthermore, x'_{it} ($i=1, 2$) also solves (R*.2) because the equality (3.7) implies that the migration term $\frac{a}{p_i}(x_{jt} - x_{it})$ vanishes in (R*.2), so that (R*.2) reduces to (F*.2). Based on uniqueness of solutions, it follows that the solution to (R*.1) is given by $N_{1t} = K_1 x'_t = p_{1t} K x'_t$ and $N_{2t} = K_2 x'_t = p_{2t} K x'_t$; consequently $N_t = K x'_t$. This proves (3.6). ■

As in Theorem 1, existence and uniqueness follow by mathematical induction for model R2, but are beyond the scope of this paper for model R1. Again, we confine ourselves to the biologically meaningful circumstances in which (R*.1) and (R*.2) have solutions that exist and are unique for specified initial conditions, as illustrated in Section 6.

4. Equilibrium Catch Calculations

From the perspective of fishermen, the ultimate value of a fishery lies in the catch produced by fishing. This corresponds to the catch rate

$$C_t = F_t N_t \quad (4.1)$$

at time t in the context of model F1 or the total catch during the time interval $(t, t+1)$ in the context of F2. An equilibrium model, obtained with a constant fishing mortality F , is often used to assess the potential of a fishery. Analytically, this produces the model obtained from (F*.1) by dropping the index t and (in the continuous-time models) setting $dN_t/dt = 0$. The resulting equation is exactly the same for both models F1 and F2. (In F2, a term N cancels from the left and right sides of the equation.)

Table 5. Equilibrium calculations from the fishery and reserve models in Tables 1 and 3.

Catch Rate from Models F1 and F2

$$F = rg(x) - M \quad (\text{EF.1})$$

$$C = KF x \quad (\text{EF.2})$$

$$C = KF g^{-1}\left(\frac{F + M}{r}\right) \quad (\text{EF.3})$$

Catch Rate from Models R1 and R2

$$x_2 = x_1 \left[1 - \frac{p_1}{a} (rg(x_1) - M) \right] \quad (\text{ER.1})$$

$$F_2 = \frac{p_1 x_1}{p_2 x_2} [rg(x_1) - M] + rg(x_2) - M \quad (\text{ER.2})$$

$$C_2 = p_2 K F_2 x_2 \quad (\text{ER.3})$$

$$g^{-1}\left(\frac{p_1 M + a}{p_1 r}\right) < x_1 < 1; \quad 0 < x_2 < x_1 \quad (\text{ER.4})$$

Table 5 shows the results of an equilibrium analysis of the fishery models in Table 1. The equilibrium version of equation (F*.1) can be solved for F to express the fishing mortality in terms of $x = N/K$, as shown in (EF1). The catch equation (4.1) expresses C in terms of x , with the result (EF.2). The state variable x can be eliminated by combining (EF.1) and (EF.2) to give the explicit representation (EF.3) for C as a function F . This involves the inverse function $g^{-1}(y)$, where $y = g(x)$. Our assumption that $g(x)$ is strictly decreasing guarantees that $g^{-1}(y)$ exists for y in the range of $g(x)$. Formula (G.3) in Table 2 explicitly shows the inverse for the

function defined in (G.1). The functions $C(F)$ in (EF.3) can be maximized to obtain harvest and catch levels that correspond to the maximum sustainable yield (MSY). From this point of view, the level of fishing mortality F serves as a control that can be adjusted to maximize C in the long run.

Table 5 also shows an equilibrium analysis for the reserve models R^* in Table 3. The results are not as tidy as those for the fishery models F^* , but they are still tractable numerically. The equilibrium version of (R*.2) with $i=1$ allows us to express x_2 in terms of x_1 , as shown in (ER.1). Similarly, the equilibrium version of (R*.2) with $i=2$ gives the expression (ER.2) for the fishing mortality F_2 in region 2 as a function of x_1 and x_2 . Finally, the catch equation (4.1) gives the catch C_2 in region 2 as a function of x_2 and the fishing mortality F_2 . In this analysis, F_2 serves as one control, and the proportion p_1 of carrying capacity set aside as a reserve serves as another. The result (ER.3) allows us to calculate C numerically as a function of (p_1, F_2) . Consequently, we can find values of these controls that maximize C . More generally, we can evaluate the trade-off between the proportion p_1 in the reserve and the fishing mortality F_2 allowed outside the reserve.

Numerically, the equilibrium calculations (ER.1)–(ER.3) start with a vector of values x_1 and proceed sequentially through three steps as follows:

$$x_1 \Rightarrow x_2 \Rightarrow F_2 \Rightarrow C_2. \quad (4.2)$$

To start this calculation, we need to choose a range for x_1 . We anticipate that the density in the reserve should be higher than in the fishery, because no fishing mortality occurs in the reserve. The condition $x_2 < x_1$ implies that a quantity contained in large square brackets in equation (ER.1) must be less than 1. Explicitly, we require that

$$1 - \frac{p_1}{a} (r g(x_1) - M) < 1.$$

This condition, in turn, implies the lower bound (ER.4) for x_1 in (ER*.d) that restricts the meaningful range of x_1 for equilibrium calculations.

Why would we expect a lower bound for x_1 ? Imagine a reserve with a very low migration rate a into the fishery. Then, even if the fishery captures all the available fish, we might still expect the reserve population to move close to carrying capacity ($x_1 \approx 1$), given only a minor “leakage” into the fishery. In fact, as $a \rightarrow 0$, the lower limit for x_1 in (ER.4) converges to 1.

5. Practical applications and software

As stated in the introduction, we’ve developed the models here explicitly to address four key questions about the impact of marine reserves. We can now reformulate these questions in more technical terms to relate them to the analyses above:

1. How do population trajectories N_i ($i=1,2$) change inside and outside a reserve after it is established?
2. How are long term catches C_2 and population levels N_i ($i=1,2$) altered by adjusting the proportion p_1 of habitat set aside in the reserve and the level of fishing F_2 in the region outside the reserve?
3. What combinations of reserve proportion p_1 and harvest level F_2 might be used to achieve social goals, such as a long term stable catch?
4. How are the answers to these questions influenced by values of the key biological parameters r, K, M, k, a , and γ ?

Question 1 is partly answered by Theorem 2. Within the framework developed here, population trajectories remain proportional to local carrying capacity until the harvest policy is changed in the reserve. After that, the trajectories diverge, and we can use simulation from the equations in Table 3 to mimic that process precisely. We should add, however, that we could alter the framework with different assumptions about the distribution of fish between fishery and the reserve. For example, we could have assumed that the reserve contains all available breeding habitats, and that larvae flow from the reserve to the fishery. Such a structural change would substantially alter the models discussed here, which assume a uniform habitat throughout the reserve and fishery.

Questions 2 and 3 are addressed by the equilibrium analyses in Table 5. We've designed the models to include two policy parameters, the proportion p_1 set aside as a reserve and the harvest level F_2 in the fishery. For example, a recipe for the equilibrium calculations based on model R1 or R2 is:

- A. Start with a grid of values (p_1, x_1) , with $0 < p_1 < 1$ and $0 < x_1 < 1$.
- B. Eliminate points from this grid that violate the constraint (ER.4).
- C. For the remaining legitimate points in the grid, perform the calculations (ER.1)–(ER.3) to obtain the results in (4.2). This gives a set of vectors $(p_1, x_1, x_2, F_2, C_2)$ that represent equilibrium states for model R1 or R2.
- D. Use the triplets (p_1, F_2, C_2) , (p_1, F_2, x_1) , and (p_1, F_2, x_2) to interpolate contour plots that relate the catch C_2 and the densities x_1 and x_2 to the control variables (p_1, F_2) .

Question 4 can be addressed by designing simulations that allow the underlying parameters (K, r, M, k, a, γ) to be altered easily. We also use sinusoidal functions

$$F_t = F_{\min} + \frac{F_{\max} - F_{\min}}{2} \left(1 + \sin \frac{2\pi t}{n} \right) \quad (5.1)$$

to represent time-varying fishing mortality, where a user can specify minimum and maximum fishing mortality levels (F_{\min}, F_{\max}) and the number n of time steps in one full cycle.

To accomplish the simulation goals outlined above, we decided to use the freely available software environment R (R Development Core Team 2006; <http://www.R-project.org>). Our

simulations require an interface that can readily be configured and modified to facilitate experimental probing. For this purpose, we first designed and produced an R library *PBS Modelling* (Schnute et al. 2006) that makes it easy to build such an interface, for this project and many others as well. Our library, now publicly available on the Comprehensive R Archive Network (CRAN, <http://cran.r-project.org/>), will eventually include this project as a special example. In that way, we intend to make our simulations available via the Internet to users worldwide.

Libraries currently available for R include *odesolve*, a package for solving ordinary differential equations (ODEs). The author (R. Woodrow Setzer) used Fortran code by Linda Petzold and Alan Hindmarsh (Lawrence Livermore National Laboratory, Livermore, California) that implements advanced algorithms for solving stiff and non-stiff ODEs. The *odesolve* library provides an R wrapper for this well-designed code so that the gradient function can be programmed in R. Given suitable code to do this, an R programmer needs only to call a special R function in the library that invokes the Fortran algorithm to perform the numerical solution.

Prior to our project, no one had made a similar R library for solving delay differential equations (DDEs), as required for our models F1 and R1. Thanks to our intrepid programmer and coauthor Alex Couture-Beil, this situation has now changed. Alex found modern C/C++ code to solve DDEs written by Simon Wood (University of Bath, Bath, UK; home page <http://www.maths.bath.ac.uk/~sw283/index.html>). Following the style of *odesolve*, Alex built an R wrapper for Simon’s code (<http://www.maths.bath.ac.uk/~sw283/simon/dde.html>) that allows the lagged gradient function to be programmed in R. Thanks to Simon’s (enthusiastic) permission to use his code in our new package, we plan to post *ddesolve* on CRAN. This will fill a notable gap in the algorithms available for R. Our simulations use *odesolve* when $k = 0$ in model R1, but switch to *ddesolve* when $k > 0$. Using a small lag k , our simulations can be used to compare results from these two algorithms.

6. Worked examples

The right panel of Figure 1 illustrates a scenario in which a reserve facilitates population recovery from overfishing. In this case, heavy fishing occurs throughout the entire fishery during the first 15 years and seriously depletes the initial population. The population remains evenly distributed between regions 1 and 2, as anticipated from Theorem 2. A reserve containing 70% of available carrying capacity is established in year 15, after which fishing stops in region 1 and heavy fishing continues in region 2 with the remaining 30% of carrying capacity. Over several decades, the stock slowly recovers and produces steady catches similar to those achieved historically during the mid-phase of the initial overfishing period.

The GUI in the left panel of Figure 1 shows the tools available in our software for exploring such possibilities. It contains three sections – Simulation, Equilibrium, and History. In “Simulation”, the user chooses biological parameters and control variables, then presses the button marked **Plot trajectories** to see how simulated reserve and fishery populations behave over time given these choices. Additionally, the button **Plot g(x)** displays the density-dependent recruitment response, given the parameters r, M , and γ .

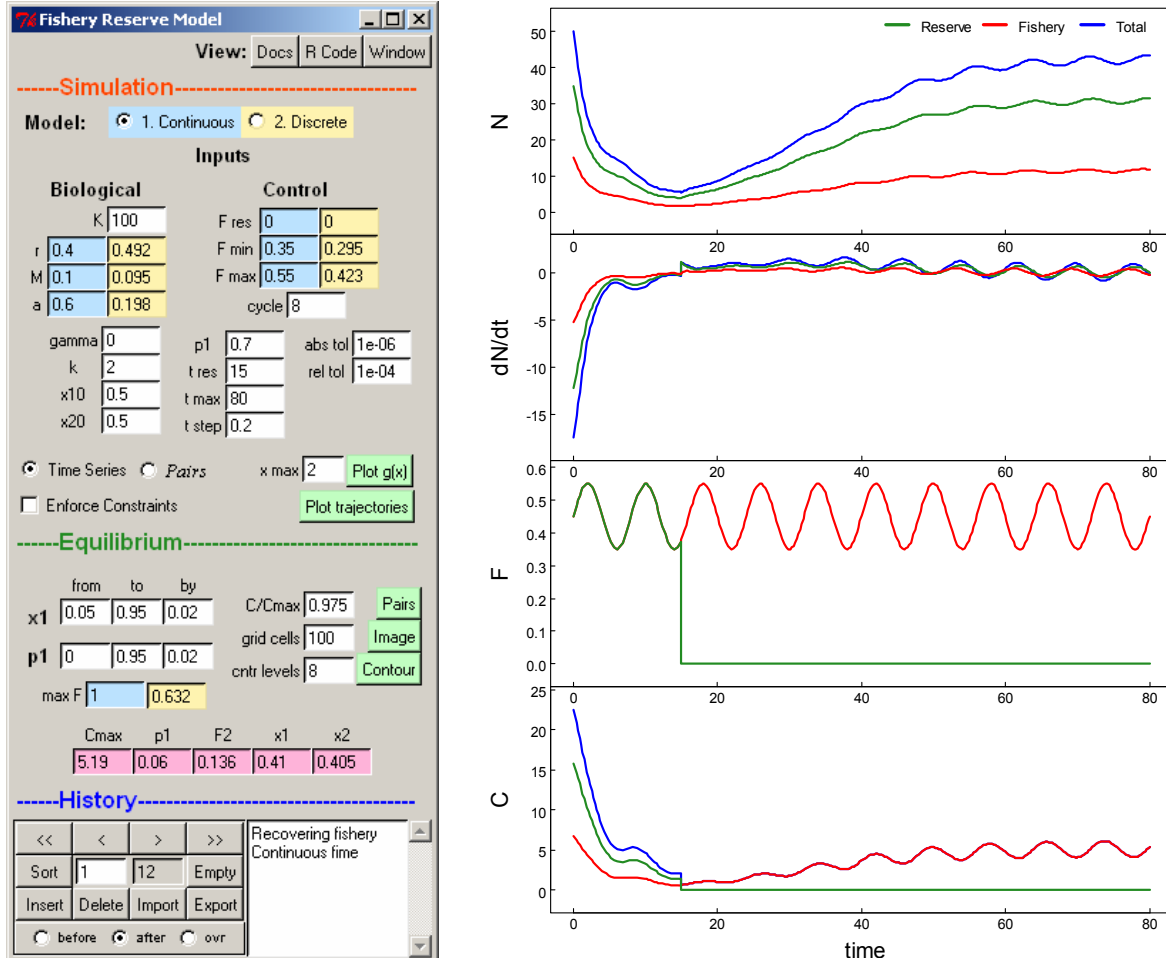


Figure 1. Recovery of a heavily fished population after establishing a reserve. **Left:** The GUI shows all input values (parameters and controls). The selected continuous time model R1 uses input values common to both models (white background) and values specific to the continuous model (blue background). Corresponding values are computed for the discrete model (yellow background) from (2.3) and (3.5). **Right:** Output trajectories trace various results (N = population, dN/dt = instantaneous change in population, F = instantaneous fishing mortality, C = instantaneous catch) for the reserve and fishery. Fishing mortality follows the sinusoid (5.1) determined by F_{\min} , F_{\max} , and the cycle length n .

The “Simulation” section of the GUI also offers a choice of two models – **Continuous** (blue shade) and **Discrete** (yellow shade). Inputs specific to either model are similarly shaded, and the equivalent values in the other shade are calculated using transformations (2.3) and (3.5) upon execution of a plot. Non-shaded input boxes are common to both models. Biological parameter constraints in Tables 1 and 3 can be enforced or not. If the box **Enforce Constraints** is checked, the code resets unsuitable parameter values upon plot execution and displays reset values in the R console window. By ignoring constraints, a user can explore scenarios outside the bounds normally expected for biological systems.

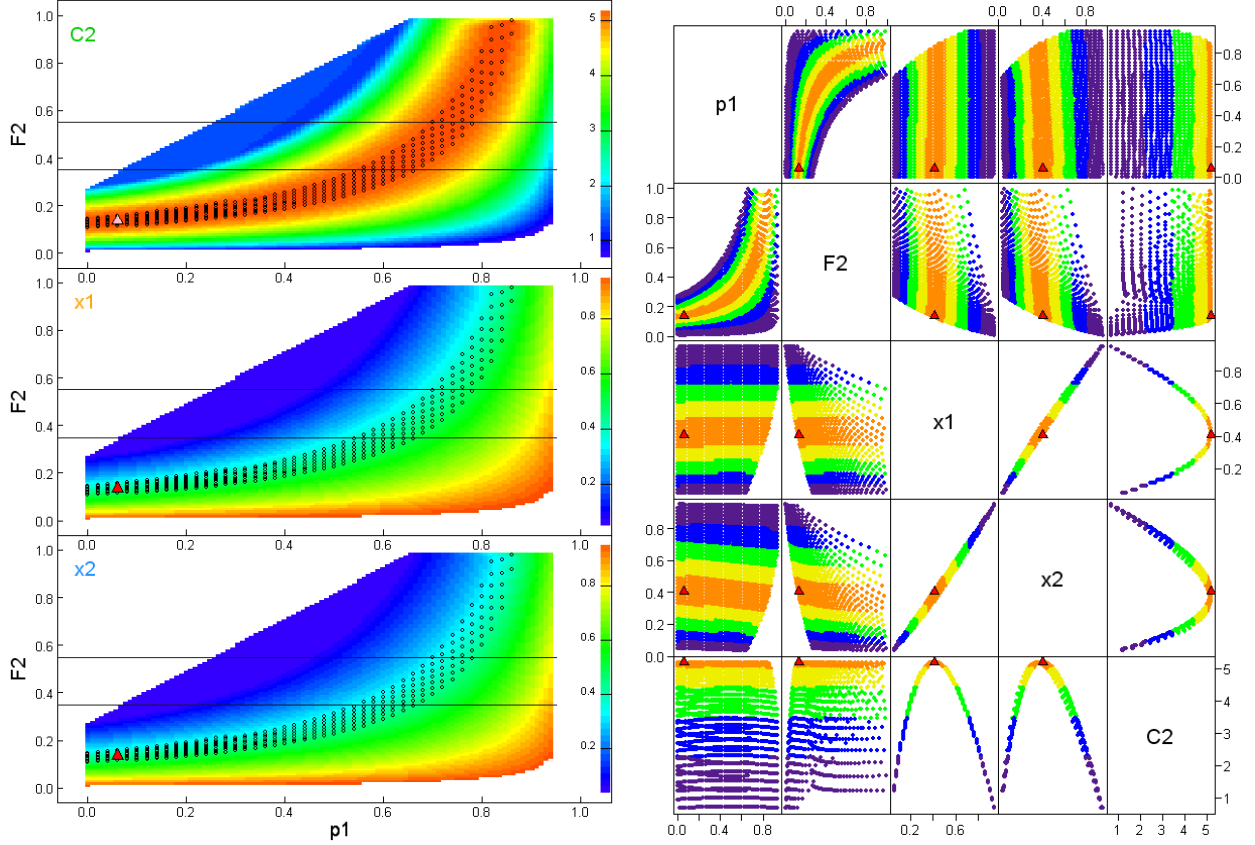


Figure 2. Equilibrium conditions for a range of values (x_1, p_1) specified in the GUI shown in Figure 1. Red triangles in all plots designate the point corresponding to the maximum catch C_{\max} . **Left:** Image plots show levels of C_2 , x_1 , and x_2 , where black circles indicate points with $C/C_{\max} \geq 0.975$. Horizontal lines delimit the controls F_{\min} and F_{\max} specified in the “Simulation” section of the GUI. **Right:** A pairs plot illustrates relationships among $(p_1, F_2, x_1, x_2, C_2)$, colour-coded by quantiles of C_2 .

The “Equilibrium” section of the GUI has additional inputs for creating a matrix of equilibrium values, based on the computations (ER.1)–(ER.4) in Table 5 with specified ranges for the vectors x_1 and p_1 . The user can visualize the resulting matrix using the buttons **Pairs** for pairs plots (Figure 2, right), **Image** for image plots (Figure 2, left), and **Contour** for contour plots (not shown here). Values from the matrix that yield the maximum equilibrium catch C_{\max} appear within the GUI as boxes shaded pink.

The “History” section of the GUI allows a user to scroll through saved sets of inputs, rather like viewing a slide show. It also facilitates the insertion, deletion, and sorting of input scenarios, just as slides might be assembled to produce a show. The resulting show can be saved as a text file and passed among users to illustrate cases of special interest. The GUI in Figure 1 (left) uses a generic “history” widget made routinely available in the *PBS Modelling* package. In addition, the software for this report includes a particular history file that assembles the input required to produce the figures shown here, along with other examples. Comments in the “History” section highlight features of interest, like notes that might accompany a slide.

We return now to the details of the example in Figures 1 and 2. Each of the four questions in the Introduction and Section 5 has an explicit answer from the analyses here.

1. *Question:* How does establishing a reserve change population trajectories?

Answer: Figure 1 shows population trajectories before and after 70% of the original fished area is set aside as a reserve in year 15. During the initial period, the total population N_t declines from 50 units to about 10 units, and (as proved in Theorem 2) the populations N_{1t} , N_{2t} and N_t maintain the constant ratio (3.6). After the reserve is established, it recovers slowly to about 40 units, with the recovery driven by a larger population N_{1t} .

2. *Question:* How do the controls (p_1, F_2) influence the long term catch?

Answer: Figure 2 explicitly relates the equilibrium catch C_2 to the proportion p_1 of habitat set aside in the reserve and the level of fishing F_2 in the region outside the reserve. The maximum sustainable catch $C_{\max} = 5.19$ occurs when $p_1 = 0.060$, $F_2 = 0.136$, $x_1 = 0.410$, and $x_2 = 0.405$.

3. *Question:* How can the controls (p_1, F_2) be adjusted to achieve social goals?

Answer: The MSY scenario mentioned in answer to question 2 may not be socially feasible. For example, it might be impossible to limit fishing mortality to the low level $F_2 = 0.136$. The manager might also consider scenarios with $C/C_{\max} \geq 0.975$ illustrated by small black circles in Figure 2 (left). For instance, in the region of a target F that lies between 0.35 and 0.55 (horizontal lines in the image plot), a high catch can still be achieved with $p_1 \approx 0.7$, as portrayed in Figure 1.

4. *Question:* How do the answers to questions 1, 2, and 3 vary with key biological parameters?

Answer: The GUI allows a user to explore how the answer to any question varies with chosen values of the biological parameters r , K , M , k , a , and γ . It also allows a choice between models with continuous or discrete time t .

Given the base case portrayed in Figures 1 and 2, the GUI allows a user to explore other possibilities. For example, Figure 3 shows what happens if the recruitment lag k increases from 2 to 25 years. An influx of recruitment from the preceding 25 years enhances the initial phase of fishery recovery. After this, the total population shows long cyclic patterns associated with long recruitment lags. This contrasts with the trajectories in Figure 1, which show relatively fast response to the sinusoidal fishing mortality F_{2t} .

A user might conduct further explorations relevant to particular species. For example, the rockfish genera *Sebastodes* typically have low reproductive growth rates r and low natural mortalities M . They also tend to remain associated with reefs and other benthic features, so that the movement parameter a would likely take a low value. Although this report can show only a few special cases, the software makes it possible to try many scenarios based on different biological systems.

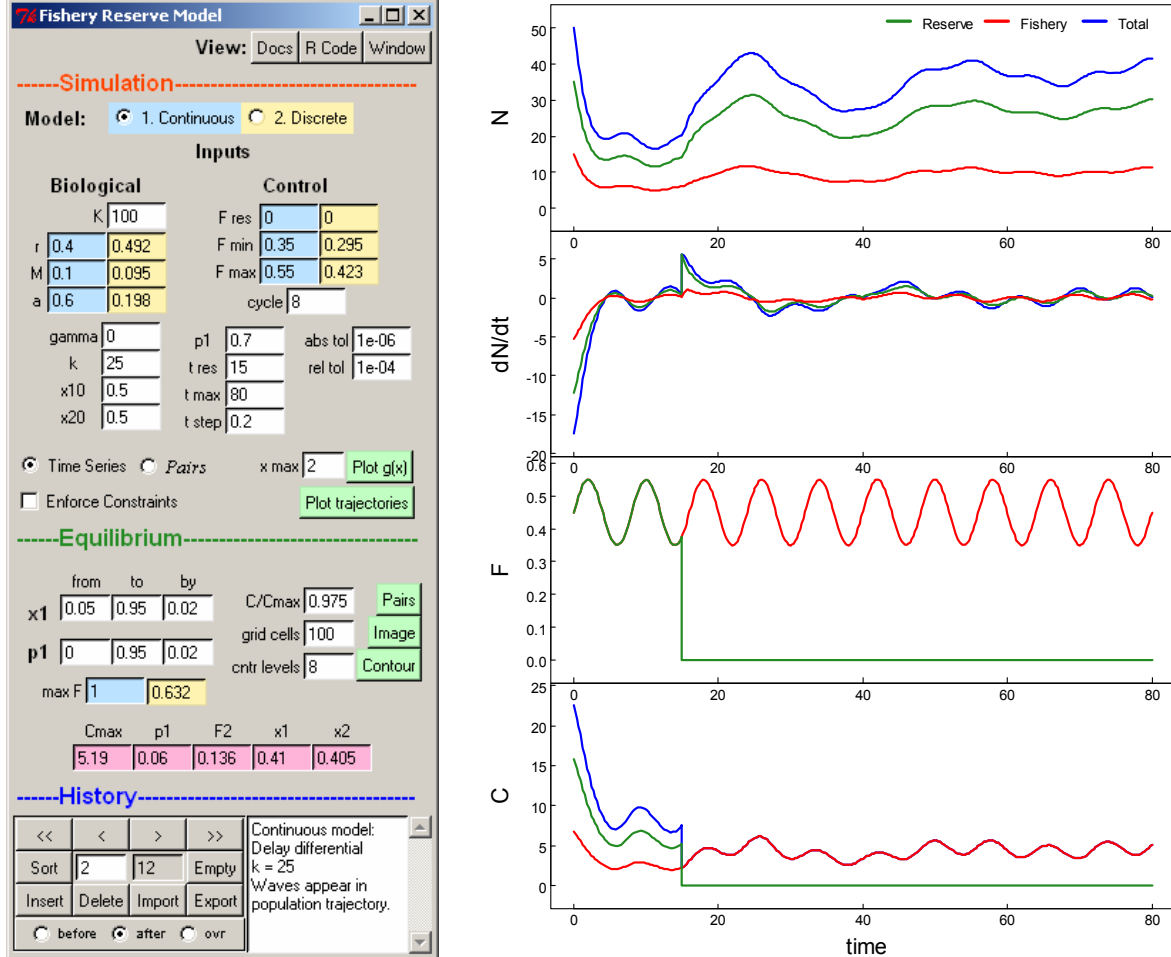


Figure 3. Recovery of a heavily fished population after establishing a reserve. All settings and explanations match those in Figures 1 and 2, except that $k = 25$. Equilibrium results shown in Figure 2 remain valid, but the trajectories here differ from those in Figure 1. **Left:** GUI with $k = 25$. **Right:** Revised trajectories, with less initial decline due to the influx of recruitment from the preceding 25 years.

The density-dependent recruitment function $g(x|r, M, \gamma)$ in Table 2 provides a way to represent the population's response to density effects. As mentioned above in Section 2, specific values of γ define classical models ($\gamma = 0$ for the Ricker and $\gamma = -1$ for the Schaeffer or Beverton-Holt.) In general, γ can take any real value, and Figure 4 portrays the density effect $g(x)$ and recruitment response $xg(x)$ for four values of γ . For increasingly negative values γ , the population becomes more sensitive to density and less able to exceed the carrying capacity K . Alternatively, the population has an increasing ability to expand beyond K as γ takes larger positive values.

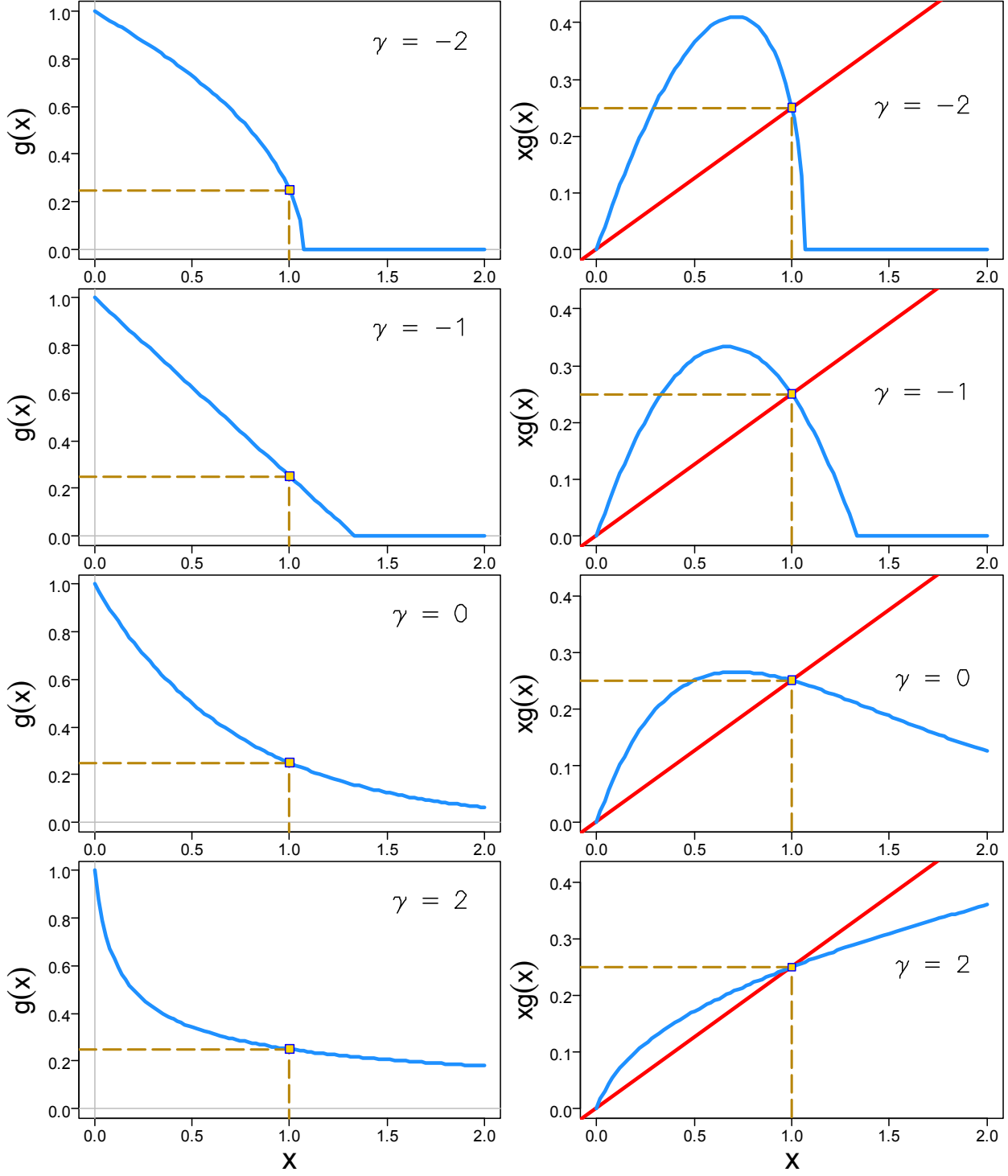


Figure 4. Density dependent recruitment response when $r = 0.4$ and $M = 0.1$, where the function $g(x | r, M, \gamma)$ is defined in Table 2. All curves pass through a point (square) determined by the constraint (F1.4) that $g(1) = M/r$. **Left:** Plots of $g(x)$ for $\gamma = -2, -1, 0, 2$. **Right:** Corresponding plots of $xg(x)$, where a red line through the origin has slope M/r .

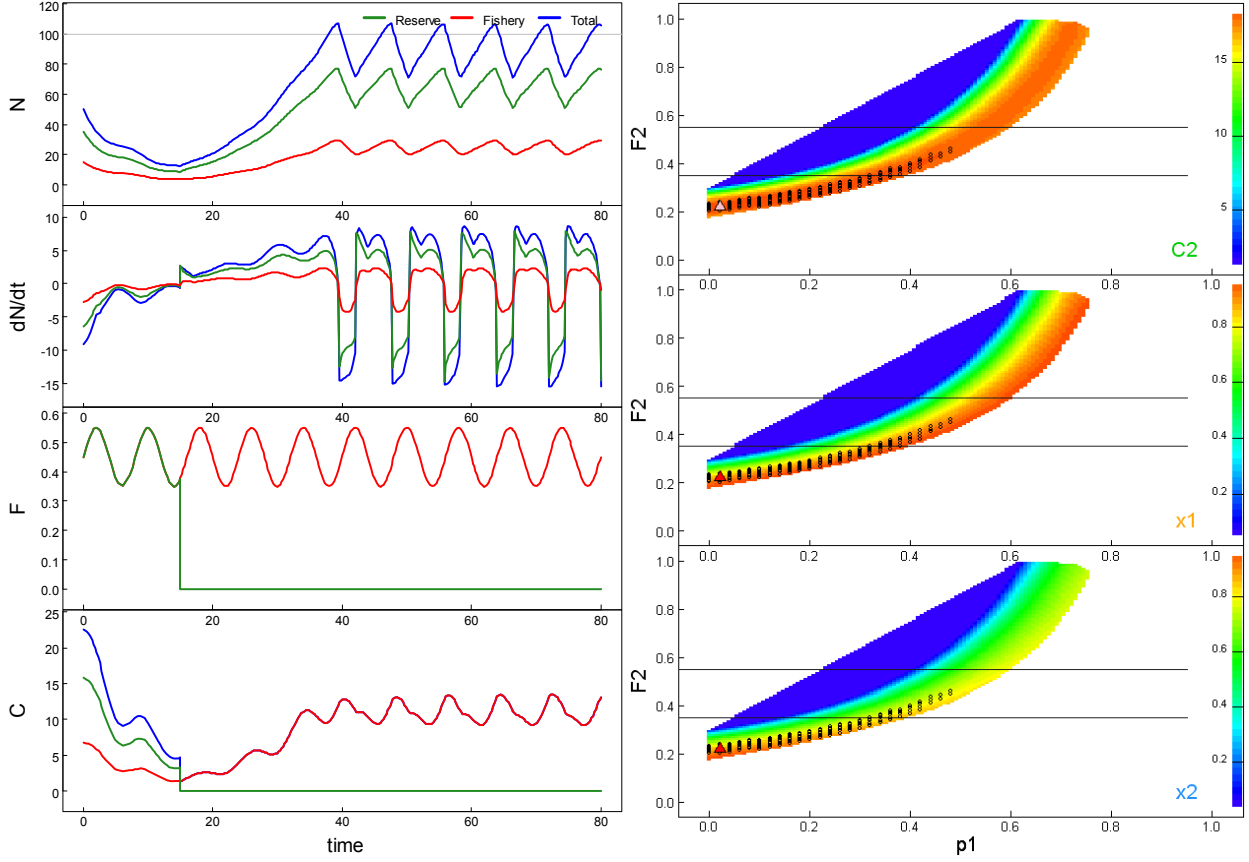


Figure 5. Recovery of a heavily fished population after establishment of a reserve. All settings and explanations match those in Figures 1 and 2, except that $\gamma = -8$. Left: The total population sometimes exceeds the carrying capacity $K = 100$ and experiences severe density-dependent recruitment failure. Right: Image plots show that the intended harvest levels F_2 between 0.35 and 0.55 do not correspond to equilibrium levels, given the specified proportion $p_1 = 0.7$ in the reserve.

Figure 5 examines the scenario of a recovering fishery in Tables 1 and 2 when $\gamma = -8$, so that the population experiences high density dependence. Time trajectories show two key features of the populations N_{1t} and N_{2t} after the reserve is established. First, they slowly recover to levels exceeding those at the start. Second, they experience sharp recruitment failures when N_{1t} and N_{2t} exceed the carrying capacities K_1 and K_2 . Given the reserve size ($p_1 = 0.7$), the fishing mortality range ($0.35 \leq F_{2t} \leq 0.55$) remains incompatible with equilibrium conditions determined by the biological parameters. The image plot in Figure 5 suggests a better policy. For the specified levels of fishing mortality, it would actually improve matters to reduce the the reserve proportion p_1 from 0.7 to a value in the range 0.4–0.5. This counterintuitive result stems from the (perhaps unrealistically) high level of density dependence when $\gamma = -8$. The density plot also shows that the condition $F_2 = 0$ is incompatible with equilibrium. Without fishing, the population experiences natural cycles (not shown), as can be observed using the GUI.

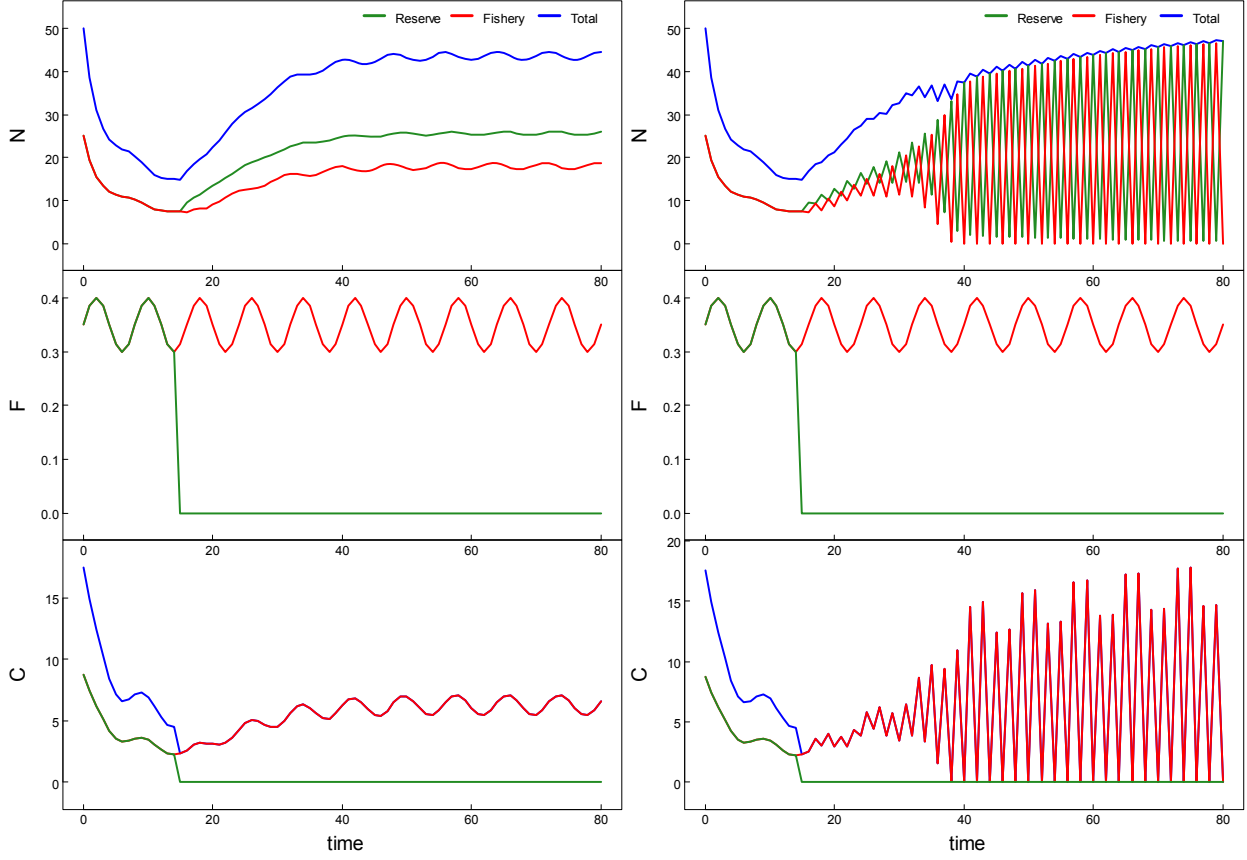


Figure 6. Trajectories generated using the discrete model (R2.1) with $K = 100$, $r = 0.5$, $M = 0.1$, $\gamma = 0$, $k = 2$, and $p_1 = 0.5$. Fishing mortality F_{2t} follows the sinusoid (5.1) with $F_{\min} = 0.3$ and $F_{\max} = 0.4$. Panels represent two values of the movement parameter a . **Left:** $a = 0.2$. **Right:** $a = 2p_1p_2 = 0.5$, the highest possible value with bounded solutions (M2.4) to the movement model (M2.1).

The discrete-time model (R2.1) behaves similarly to the continuous model (R1.1), except for extreme values of the movement parameter a . Solutions (M2.4) to the discrete movement model (M2.1) have (i) non-oscillatory, (ii) bounded oscillatory, and (iii) unbounded oscillatory behaviour for values a in the ranges (i) $0 \leq a \leq p_1p_2$, (ii) $p_1p_2 < a \leq 2p_1p_2$, or (iii) $p_1p_2 < a$. Our reserve models (R2.1) generally inherit this qualitative behaviour from the movement component, although we constrain our solutions so that N_{1t} and N_{2t} never become negative. Figure 6 shows results from (R2.1) for two values of a , where (left) $a < p_1p_2$ and (right) $a = 2p_1p_2$. In the latter case, high oscillations between N_{1t} and N_{2t} produce a relatively stable total population $N_t = N_{1t} + N_{2t}$. According to this model, the population shifts rapidly between the reserve and the fishery at each time step. Probably this is highly unrealistic, but strange things sometimes happen in nature. Exercises like this one can alert users to possibilities that otherwise might never have been considered.

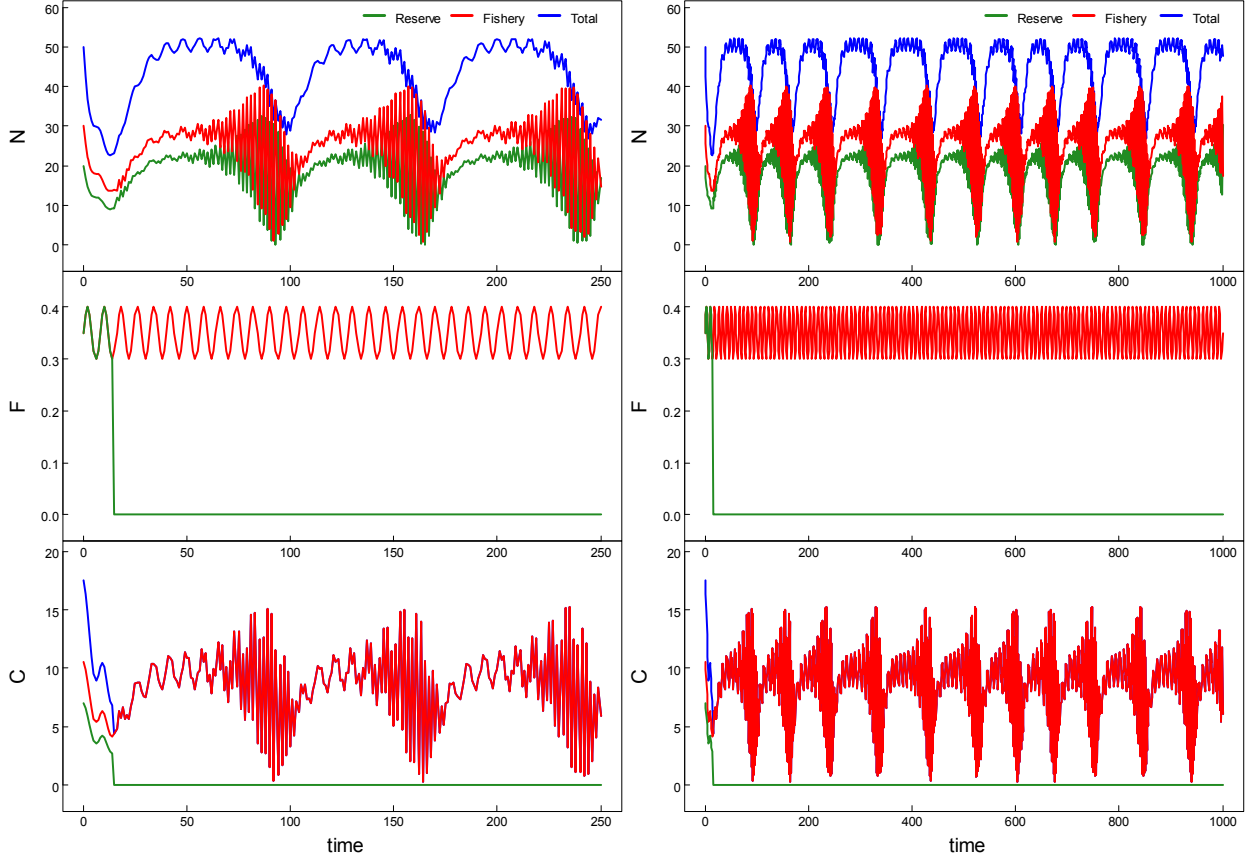


Figure 7. Chaotic long-term trajectories for the discrete model R2 with $K = 100$, $r = 0.5$, $M = 0.1$, $\gamma = -1$, $k = 2$, $a = 0.458$, $p_1 = 0.4$, $F_{\min} = 0.3$, and $F_{\max} = 0.4$. **Left:** Results for 250 years. **Right:** Results for 1,000 years.

Figure 7 illustrates another extreme result from the discrete model (R2.1). In this case, a fairly sensitive density response ($\gamma = -1$) interacts with a high value of the movement parameter $a = 0.458 < 2p_1p_2 = 0.48$ to produce an interesting long term chaotic pattern. High production levels occur episodically for variable periods of time. Similar patterns sometimes appear in ocean production data or even financial data from the stock markets. Our deterministic model might potentially be used to generate pseudo-random variables with desired temporal properties. This example touches on the science fiction concepts mentioned in the Introduction. Ideas conceived in one context may produce surprising results that have potential applications in entirely different fields.

7. Discussion

Our models represent fishery reserves rather simplistically in terms of four fundamental processes: birth, natural mortality, fishing mortality, and the movement of fish between two regions. Mortality and movement follow linear models, with rates proportional to the available populations. The mortality components imply simple exponential decay, and Table 4 gives explicit solutions to the movement component of the model. Nonlinear behaviour enters the

analysis only in the birth component of the model, as illustrated in the right-hand panels of Figure 4. Nonlinear properties of the function $xg(x)$ give the population a limiting size, where abundance tends toward the carrying capacity K in the absence of fishing. We allow a time lag of k years between the birth of larval fish and their appearance as adults at age k . (Note that our notation is case sensitive; K and k have entirely different meanings.)

Despite their relative simplicity, our models demonstrate chaotic behaviour for certain parameter values. This result can be anticipated for discrete-time models with shape parameters $\gamma < 1$ that correspond to dome-shaped curves in Figure 4 (right panels). In such cases, recursive functions (like the Ricker function $xg(x|\gamma)$ with $\gamma = 0$) in the basic fishery model (F2.1) have known chaotic properties (Kuznetsov 1995, p. 114; Schnute 2006). We have extended this result to reserve models (R2.1), where the movement parameter a interacts with γ and other parameters. Chaotic behaviour stems partly from oscillating solutions (M2.4) to the movement component of a reserve model, as illustrated in Figures 6 and 7.

We handle uncertainty only in the naïve sense of exploring how different parameter values influence a deterministic model. Because stochastic error can't readily be introduced into delay-differential equations, a modern fishery model would more typically use only a discrete-time formulation with stochastic error at each time step. This could include error in each of the underlying processes: birth, mortalities, and movement. The parameters (K, r, M, γ, a), which are assumed constant here, might also be modelled as random variables.

We could also change key structural assumptions, such as the spatial distribution of larvae or the age composition of the population. We could formulate the model in terms of biomass, rather than abundance, and include another model component related to fish growth. We could increase the number of regions and explore consequences of setting aside different areas as reserves. Any such change could potentially give substantially different conclusions from those described here.

We have not addressed the important issue of response by fishermen to a restricted area of fishing. In our models, a user can easily test hypothetical control variables (p_1, F_{2t}), but this exploration glosses over important social issues related to compliance and enforcement. For example, poachers might catch fish illegally in the reserve, or fishermen might not respect the measures needed to restrict fishing mortality. Extensions of the model could investigate such scenarios by adding functions that predict responses by fishermen and the general public to new reserve policies. An objective function tuned to social goals might also be used to assess formally the model results.

In practice, our models would need to be customized for a particular context, and stakeholders would need to become directly involved. Simulations like those illustrated here could facilitate the development of policies that will be implemented successfully. Management starts with planning, and the R software described here offers a freely available tool for designing interactive studies of fishery reserves and other ecological systems.

References¹

- Beverton, R.J.H., and Holt, S.J. (1957) On the dynamics of exploited fish populations. UK Ministry of Agriculture, Fisheries and Food. *Fisheries Investigation Series 2*, No 19.
- Gaines, S.D., Gaylord, B., and Largier, J.L. 2003. Avoiding current oversights in marine reserve design. *Ecological Applications* 13: S32-S46.
- Gerber, L.R., Botsford, L.W., Hastings, A., Possingham, H.P., Gaines, S.D., Palumbi, S.R., and Andelman, S. 2003. Population models for marine reserve design: a retrospective and prospective synthesis. *Ecological Applications* 13: S47-S64.
- Halpern, B.S. 2003. The impact of marine reserve: do reserves work and does reserve size matter? *Ecological Applications* 13: S117-S137.
- Halpern, B.S. and Warner, R.R. 2002. Marine reserves have rapid and lasting effects. *Ecology Letters* 5: 361-366.
- Hastings, A., and Botsford, L.W. 1999. Equivalence in yield from marine reserves and traditional fisheries management. *Science* 284: 1537–1538.
- Kuznetsov, Y.A. 1995. Elements of applied bifurcation theory. *Applied Mathematical Sciences*, Vol. 112. Springer-Verlag. New York. 515 pp.
- Pauly, D., Palomares, M.L., Froese, R., Sa-a, P., Vakily, M., Preikshot, D., and Wallace, S. 2001. Fishing down Canadian aquatic food webs. *Canadian Journal of Fisheries and Aquatic Sciences* 58: 51-62.
- Pella, J.J., and Tomlinson, P.K. 1969. A generalized stock production model. *Inter-American Tropical Tuna Commission Bulletin*, 13(3): 419–496.
- R Development Core Team. 2006. R: A language and environment for statistical computing. R Foundation for Statistical Computing, Vienna, Austria. ISBN 3-900051-07-0, URL <http://www.R-project.org>.
- Ricker, W.E. 1954. Stock and Recruitment. *Journal of the Fisheries Research Board of Canada* 11: 559-623.
- Ricker, W.E. 1975. Computation and interpretation of biological statistics of fish populations. *Bulletin of the Fisheries Research Board of Canada*, No. 191. 382 pp.
- Shea, K., et al. 1998. Management of populations in conservation, harvesting and control. *Trends in Ecology and Evolution*, 13(9): 371-375.
- Schaefer, M.B. 1954. Some aspects of the dynamics of populations important to the management of the commercial marine fisheries. *Inter-American Tropical Tuna Commission Bulletin*, 1: 25–56.
- Schaefer, M.B. 1957. A study of the dynamics of the fishery for yellowfin tuna in the eastern tropical Pacific Ocean. *Inter-American Tropical Tuna Commission Bulletin*, 2: 245–285.
- Schnute, J.T. 2006. Curiosity, recruitment, and chaos: a tribute to Bill Ricker's inquiring mind. *Environmental Biology of Fishes* 75: 95–110.

¹ For the reader's convenience, we include some useful references that are not explicitly cited in the text.

- Schnute, J.T., Boers, N.M., and Haigh, R. 2003. PBS software: maps, spatial analysis, and other utilities. Canadian Technical Report of Fisheries and Aquatic Sciences 2496. viii+82 pp.
- Schnute, J.T., Boers, N.M., and Haigh, R. 2004. PBS Mapping 2: user's guide. Canadian Technical Report of Fisheries and Aquatic Sciences 2549. viii+126 pp.
- Schnute, J.T., Couture-Beil, A., and Haigh, R. 2006. PBS Modelling 1: User's Guide. Canadian Technical Report of Fisheries and Aquatic Sciences 2674: viii + 114 p.
- Schnute, J.T., and Richards, L.J. 2002. Surplus production models. Chapter 6, p. 105–126. In: Hart, P.J.B., and J.D. Reynolds. Handbook of Fish Biology and Fisheries, Volume 2: Fisheries. Blackwell Science Ltd. Oxford, UK.
- Worm, B., Barbier, E.B., Beaumont, N., Duffy, J.E., Folke, C.F., Halpern, B.S., Jackson, J.B.C., Lotze, H.K., Micheli, F., Palumbi, S.R., Sala, E., Selkoe, K.A., Stachowicz, J.J., and Watson, R. 2006. Impacts of biodiversity loss on ocean ecosystem services. *Science* 314: 787-790.